HHS Public Access

Author manuscript

J Phys Chem B. Author manuscript; available in PMC 2023 March 02.

Published in final edited form as:

J Phys Chem B. 2022 January 27; 126(3): 679–690. doi:10.1021/acs.jpcb.1c08157.

Human γS-Crystallin Resists Unfolding Despite Extensive Chemical Modification From Exposure To Ionizing Radiation

Brenna Norton-Baker[†,‡], **Megan A. Rocha**[†,‡], **Jessica Granger-Jones**[‡], **Dmitry A. Fishman**[‡], **Rachel W. Martin**[‡,¶]

[†]These authors contributed equally.

[‡]Department of Chemistry, University of California, Irvine, CA 92697-2025, USA

[¶]Department of Molecular Biology and Biochemistry, University of California, Irvine, CA 92697-3900, USA

Abstract

Ionizing radiation has dramatic effects on living organisms, causing damage to proteins, DNA, and other cellular components. γ radiation produces reactive oxygen species (ROS) that damage biological macromolecules. Protein modification due to interactions with hydroxyl radical is one of the most common deleterious effects of radiation. The human eye lens is particularly vulnerable to the effects of ionizing radiation, as it is metabolically inactive and its proteins are not recycled after early development. Therefore, radiation damage accumulates and eventually can lead to cataract formation. Here we explore the impact of γ radiation on a long-lived structural protein. We exposed the human eye lens protein γ-crystallin (HγS) to high doses of γ radiation and investigated the chemical and structural effects. HγS accumulated many post-translational modifications (PTMs), appearing to gain significant oxidative damage. Biochemical assays suggested that cysteines were affected, with the concentration of free thiol reduced with increasing γ radiation exposure. SDS-PAGE analysis showed that irradiated samples form protein-protein crosslinks, including non-disulfide covalent bonds. Tandem mass spectrometry on proteolytic digests of irradiated samples revealed that lysine, methionine, tryptophan, leucine, and cysteine were oxidized. Despite these chemical modifications, HγS remained folded past 10.8 kGy of γ irradiation as evidenced by circular dichroism and intrinsic tryptophan fluorescence spectroscopy.

Graphical Abstract

rwmartin@uci.edu .

Conflict of interest

The authors declare that they have no conflict of interest.

Accession Codes

Human γS-crystallin - Uniprot: CRYGS_HUMAN, PDB ID: 2M3T, 6FD8

Supplementary Information A pdf containing additional experimental results is available.

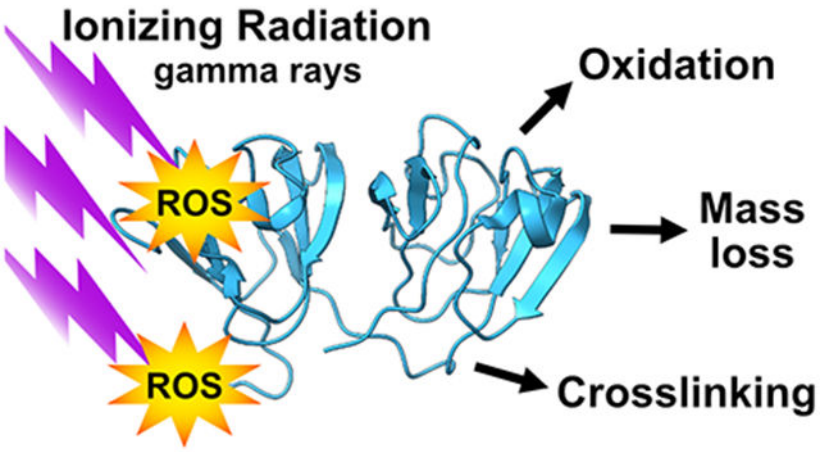

Introduction

Protein stability and aggregation resistance are intimately connected with solvent interactions. Hydrophobic hydration in general is more complicated than the traditional “oil and water” picture suggests, as the balance between attractive and repulsive interactions depends on molecular size and geometry as well as solute polarity. [1] Vibrational spectroscopy has established that at low to moderate temperatures, water assumes a structure with more tetrahedral order and fewer weak hydrogen bonds around hydrophobic solutes than the bulk solution,[2] although dangling O-H bonds are also observed near solvated hydrocarbons. [3] Exposed hydrophobic functional groups can also form highly flexible π-hydrogen bonds, where the donor is a water and the acceptor is the π-system of the aromatic amino acid side chain.[4] Microscopic interactions between water and the heterogeneous functional groups of protein surfaces impact many protein properties beyond solubility, including diffusion of water near the protein surface, [5-7] the compressibility[8] and even the refractive index increment. [9]

Water is not just a passive solvent within cells, but is a key participant in many biochemical reactions. [10] Water facilitates electron transfer in enzymes, mediating tunneling between adjacent molecules [11] or stabilizing radical intermediates in the active site [12] via hydrogen bonding. In the type of radiation damage investigated here, water acts as a transmission medium for oxidative damage: direct damage of proteins by γ rays is a minor effect, with most of the deleterious modifications coming from reactions with reactive oxygen species (ROS) derived from water, primarily hydroxyl radical, although hydrogen peroxide is also significant. [13] Inside the cell, OH radical is particularly damaging, as it is highly reactive and cannot be neutralized enzymatically, unlike H_2O_2.[14] Although DNA damage is often emphasized in studies of radiation toxicity, proteins are oxidized by hydroxyl radical before DNA or lipids. [15] The resulting protein hydroperoxide species can last for several hours and have the capacity to damage other molecules and deplete the cellular supply of antioxidants. [16] Assessing the impact of radiation damage is important for understanding the mechanisms of radiation tolerance in extremophiles, [17,18] the cellular damage caused by radiation therapy for cancer,[19] and the potential for cataract formation as a consequence of ionizing radiation absorbed by the eye.

Exposure to ionizing radiation has been shown to cause cataract in humans and model organisms.[20] Populations susceptible to radiation cataract include radiological technicians,[21] astronauts[22] and others who have accidental, occupational, or war-related exposure to ionizing radiation.[23-25] The upper dose limits of γ irradiation to the lens suggested to prevent the onset of cataract are as low as 0.05 Gy over 5 years.[26,27] These findings raise the question of whether radiation-induced cataract is a direct consequence of protein modification and aggregation or whether more complicated cellular damage is involved. The majority of the lens protein content comprises α- β- and γ- crystallins.[28] β- and γ- crystallins are structural proteins, whereas α-crystallins act as molecular chaperones. Studies on α- crystallins have shown that γ irradiation forms oxidation products, generates extensive cross-linking, damages the overall fold, and reduces chaperone activity. A previous investigation showed that rat lenses dosed with 5 Gy of γ radiation formed site-specific oxidations on γ- crystallins, particularly on cysteines, tryptophans, and methionines.[29,30] Antioxidants such as vitamin E[31,32] and melatonin[33] have delayed the onset of radiation-induced cataract in model organisms, further supporting an important mechanistic role for ROS.

Here we investigate resistance to unfolding of human γS-crystallin (HγS), a major structural protein of the eye lens, upon exposure to γ radiation. Structural crystallins such as HγS are extremely stable and soluble, in keeping with their biological role. The vertebrate eye lens is primarily composed of enucleated lens fiber cells that undergo degradation of internal organelles during early development, in part due to lipase activity[34] and the ubiquitin-proteasome system.[35] The loss of most cellular components leaves behind a highly concentrated (> 400 mg/mL) solution of proteins, mostly crystallins.[28] Crystallin solubility persists despite damage caused by aging, exposure to ultraviolet (UV) radiation, modification by reactive oxygen species (ROS), and other deleterious chemical reactions.[36,37] Glutathione and other antioxidants provide some protection from ROS,[38] however many post-translational modifications (PTMs) have been observed in aged lenses, including deamidation and oxidation.[39,40]

The aggregation resistance of the proteins themselves is partly due to fluorescence quenching mechanisms that quickly relax excited states via thermal motion before photochemistry can occur.[41-43] This wealth of information about aggregation resistance in structural crystallins leads to questions about the response of these highly soluble proteins to radiation damage, which has been shown to cause cataract: are structural crystallins such as HγS resistant to aggregation upon exposure to ionizing radiation? If they are, is it a result of increased resistance to oxidative damage or because the proteins are able to tolerate a high level of chemical modification while remaining soluble? Our results indicate that HγS is unusually robust to unfolding even when treated with high levels of γ radiation and that this resistance is due to its high tolerance for modification rather than resistance to oxidative damage. We also investigate the identity of the PTMs caused by irradiation of HγS and discuss future directions for investigation.

Materials and methods

Protein expression and purification

Human γS-crystallin (HγS) was produced using a construct containing an N-terminal 6 × His tag and a TEV cleavage sequence (ENLFQG), which leaves a glycine in place of the initiator methionine. This gene was cloned into a pET28a(+) vector (Novagen, Darmstadt, Germany) and overexpressed in Rosetta (DE3) *E. coli* cells using Studier's autoinduction protocol. [44] Cell pellets were collected via centrifugation at 4,000 rpm for 30 minutes, resuspended, lysed, and respun at 14,000 rpm for 60 minutes. The protein was purified via nickel affinity chromatography, digestion with TEV protease (produced in-house), a second round of nickel affinity chromatography (to remove the cleaved His tag), and finally, size exclusion chromatography (SEC) on a GE Superdex 75 10/300 (GE Healthcare, Pittsburgh, PA). All samples were dialyzed into H_2O, lyophilized for storage at −80 °C, and resuspended in H_2O unless otherwise stated.

γ irradiation

Protein solutions at 5 mg/mL in water (100 μL) in glass vials were irradiated with a ^{137}Cs source (^{137}Cs Irradiator Mark-I, Model 68, JL Shepherd & Associates, San Fernando, California, USA). Sample concentration was determined from the absorbance at 280 nm using an extinction coefficient of 42,860 M^{-1} cm^{-1}. Post-exposure concentrations were calculated from the final volume after sample dilution or concentration using 5 mg/mL as the known starting concentration. A metal sample holder was used to maintain consistent sample distance from the source. The dose rate has been previously calibrated with Fricke dosimetry. [45,46] Fricke dosimetry was used to confirm the expected dose for our sample position, volume, and vials. [47] Solutions of 0.4 M sulfuric acid, 6 mM ammonium ferrous sulfate and 1 mM potassium chloride were well-agitated for aeration and irradiated for 5 and 10 minutes. The absorbance at 304 nm was measured and the dose was calculated using a G-value of 15.5 mol/100 eV, extinction coefficient of 2022 M^{-1} cm^{-1}, a density of 1.024 g mL^{-1} and a path length of 1 cm. [48] The calculated dose rate at our sample position was 1.54 kGy/hr, matching the expected dose rate. Unless otherwise noted, all data were collected within 12 h of removal from the γ irradiation source.

Ultraviolet (UV) irradiation

For both UVA and UVB exposure, protein solutions were 6 mg/mL in 10 mM HEPES, 50 mM NaCl, pH 7. Sample volume was 2.5 mL in a 1 cm × 1 cm quartz cuvette. Samples were continuously stirred and temperature controlled at 22 °C using a Quantum Northwest Luma 40/Eclipse with a Peltier element and recirculator (Quantum Northwest Inc., Liberty Lake, WA, USA). For UVA exposure, a 10 Hz Nd:YAG laser (Continuum Surelite II; Surelite, San Jose, CA, USA) was coupled to a Surelite Separation Package (SSP) 2A (Surelite) to change the pump laser wavelength (1064 nm) to 355 nm via third harmonic generation. The laser flux was 29 mJ/cm^2 at 10 Hz. Samples were exposed for 180 min. For UVB exposure, a 70 mW light emitting diode (LEUVA66H70HF00, Seoul, Korea) at 5 mm distance (120 degree view angle) was used, yielding a mean power density of 58 mW/cm^2. Samples were exposed for 90 min.

SDS-PAGE

20 μL of protein was mixed with 20 μL of loading dye (62.5 mM Tris-HCl, 2% sodium dodecyl sulfate (SDS), 25% glycerol, 0.01% bromophenyl blue, pH 6.8). For reduced samples, 1 μL β-mercaptoethanol was added and samples were heated at 70 °C for 90 seconds. Samples were run on a 15% polyacrylamide gel at 180 V for 60 minutes and stained using Coomassie blue dye.

Ellman's assay

To evaluate the amount of solvent-exposed thiols in solution, the non-irradiated and irradiated protein solutions were diluted to 0.5 mg/mL in 100 mM Tris pH 8.0. 5,5′-dithiobis(2-nitrobenzoic acid) (DTNB) was added to reach a final concentration of 0.1 mM. The solutions were incubated at room temperature for 30 minutes before collection of spectra on a Jasco V-730 spectrophotometer (JASCO, Easton, MD). A molar extinction coefficient for thiobis(2-nitrobenzoic acid) (TNB) of 14150 M^{-1} cm^{-1} was used to calculate the concentration of sulfhydryl groups. [49,50]

Circular dichroism (CD)

Circular dichroism (CD) spectra were collected using a J-810 spectropolarimeter (JASCO, Easton, MD). Spectral bandwidth was set to 2 nm. All samples were diluted to 0.1 mg/mL.

Intrinsic fluorescence

Fluorescence spectra were measured using an Agilent Cary Eclipse fluorescence spectrophotometer with excitation at 295 nm. All samples were diluted to 0.1 mg/mL.

Raman

Raman studies were perform using a Raman microscope system based on a Renishaw InVia microscope. The sample was excited with a 532 nm laser (<3 mW) and spectra were collected using grating of 2400 gr/mm and under 20 s exposure time. Sample concentration was 100 mg/mL. 4 μL of sample was deposited on a glass slide and a spacer and glass coverslip was added to prevent dehydration.

Fourier-transform infrared spectroscopy (FTIR)

FTIR spectra of lyophilized protein samples were measured using a Jasco FT/IR-4700 (JASCO, Easton, MD) equipped with .in attenuated total reflection geometry fashion using ATR PRO ONE over the 400-4000 cm^{-1} range with 2 cm^{-1} resolution.

Proteolytic digestion

For samples exposed to γ-irradiation for 1 hour, digestion was performed on an aliquot of the water-soluble portion of the irradiated samples, as no significant pellet was observed upon centrifugation. For samples exposed to γ-irradiation for 5 hours as well as for the UV irradiated samples, the samples were centrifuged at 13,000 x g for 15 min and the water-insoluble fractions resolubilized in 8 M urea, 1 M ammonium bicarbonate pH 8.0. For trypsin digestion, the protein samples were denatured in 8 M urea, 1 M ammonium bicarbonate pH 8.0 for 1 h at 37 °C. The buffer was diluted or buffer exchanged to 1.6 M

urea and trypsin was added in a 1:20 ratio. The digest was carried out overnight at 37 °C. Immediately prior to analysis, DTT was added to 10 mM and the sample was heated at 80 °C for 3 minutes. For pepsin digestion, the sample was exchanged into approximately 1% formic acid (pH 1.6) and pepsin was added in a 1:20 ratio. Samples were incubated at 37 °C for 2 hours.

Liquid chromatography - mass spectrometry (LC-MS)

Mass spectra were collected on a Waters Xevo XS-QTof using either a phenyl column for intact protein mass spectra or a C4 column for peptide digests. Buffer A was 0.1% formic acid in water. Buffer B was 100% acetonitrile. For the protein intact mass spectra, the flow rate was 0.2 mL/min with a gradient of 0% to 97% B over 1.5 min then 97% B for 0.5 min. For the peptide digest mass spectra, the flow rate was 0.3 mL/min with a gradient of 3% to 27% B over 24.0 min, a gradient of 27% to 90% B over 3.0 min, then 90% B for 0.5 min. Intact mass spectra were analyzed using MassLynx with MaxEnt1 used to deconvolute the spectra. Peptide digests were analyzed with BioPharmaLynx.

Results and discussion

HγS was irradiated in a ^{137}Cs γ source at 5 mg/mL in glass vials (Figure S1). The samples are positioned equidistant in a ring around the sample source and the dose rate at this distance has been previously calibrated. [46] We confirmed our samples were receiving the expected dose using Fricke dosimetry (Figure S1).

HγS resists unfolding after high doses of γ irradiation

We used circular dichroism (CD) spectroscopy and intrinsic tryptophan fluorescence to assess the extent of unfolding in irradiated HγS. We aimed to determine whether HγS undergoes structural changes after irradiation that may be linked to radiation-induced cataract. Both the CD and fluorescence measurements indicate that HγS is remarkably resistant to unfolding upon even prolonged γ irradiation.

The CD spectra of proteins exhibit characteristic bands that report on secondary structure. [51] Here we compare the CD spectra of non-irradiated HγS to irradiated samples to detect partial or complete unfolding. In previous studies of HγS, even small changes in secondary structure due to mutation or partial unfolding were observable, i.e. as frequency shifts and shoulders on the major peaks. [52,53] For γ irradiated HγS, the CD spectra of all samples up to 10.8 kGy show a strong negative peak at 218 nm, which is characteristic of the primarily β-sheet structure of this protein (Figure 1A). At 33.9 kGy there is a loss of negative intensity at this position and broadening of the negative band toward 204 nm, where there is a new peak minimum. Similar shifting and broadening of the CD minimum at 218 nm was previously observed for γ-crystallins denatured with guanidine hydrochloride. [54] The same trend was observed for HγS that was aggregated through incubation with copper and resolubilized, [55] as well as for UV-C irradiated, aggregated, and resolubilized HγD. [56] In a previous study of human αA- and αB- crystallin, molecular chaperone proteins that are also abundant in the lens, CD was used to monitor secondary structure as these proteins were subjected to increasing doses of γ irradiation. The secondary structures of αA- and αB-

crystallin were disrupted at a dose of 3.0 kGy and 1.0 kGy of irradiation, respectively. [57] In contrast, here we show that the solubility and secondary structure of HγS is preserved up to at least 10.8 kGy.

For γ-crystallins in particular, intrinsic tryptophan fluorescence provides a nuanced view of the protein's folding state. Here we corroborated the CD results with fluorescence spectra collected over the same time course. The most obvious change in these spectra is the decrease in fluorescence intensity as irradiation increases. The arrangement of the buried tryptophans in the core of HγS has a powerful quenching effect on fluorescence; therefore, full denaturation typically increases the fluorescence signal. [43] However, other effects can alter tryptophan fluorescence intensity in the absence of full unfolding, such as transient contact with solvent molecules as a result of secondary structure destabilization [58] or modifications that alter the chemical structure of tryptophan such as conversion of tryptophan to kynurenine or other oxidation products. [59]

The position of the emission maximum is more straightforward to interpret: previous work has shown shown that the fluorescence emission maximum of β- and γ-crystallins shifts from approximately 325 nm to 340 nm when the protein is fully denatured. [60,61] Displacement of the typically buried tryptophans through denaturation exposes the residues to the more polar solvent, causing a redshift in fluorescence emission maxima upon excitation at 295 nm. [62] Partial unfolding or increased molecular motions increase the solvent accessibility of the tryptophans, leading to shifts in the spectra of a few nm. [53] The fluorescence maximum of HγS remains at 329 nm, consistent with a fully folded protein, through 10.8 kGy of irradiation (Figure 1B). After 33.9 kGy, the peak shifts from 329 to 332 nm. The CD spectra and fluorescence data both indicate that the structure of HγS is unperturbed past 10.8 kGy of γ irradiation.

Human γS-crystallin accumulates mass modifications after γ irradiation

Chemical alteration of crystallins has previously been observed after aging as well as exposure to UV light and lens contaminants such as metal cations. The best-characterized PTM of structural crystallins is deamidation, [37,63] which lowers stability and alters dynamics, potentially generating aggregation-prone transient conformations. [64,65] Oxidation is another common PTM, particularly in aged lenses that have reduced antioxidant levels. Residues that are particularly vulnerable to oxidation include cysteine, methionine, histidine, and tryptophan. [36,66] ROS formation in the lens can result from exposure to light in the UVA [67] or UVB[68] parts of the solar spectrum. Damage to biomolecules can also be caused by Fenton chemistry, where hydrogen peroxide induces redox cycling of certain metal ions (canonically, Fe^{2+} to Fe^{3+}, but also Cu^{+} to Cu^{2+}), forming hydroxyl radical and other highly reactive species. [69-72]

Despite its remarkable resistance to unfolding, HγS accumulates many mass modifications from γ irradiation. Intact mass spectra were obtained to determine if any modifications to the protein mass occurred during irradiation (Figure 2). HγS has an expected intact mass of 20932 Da, which appeared in the purified protein spectrum shown in Figure 2 (top). During irradiation, a number of mass modifications accumulated that led to both increases

and losses in mass. Mass increases appear to be mostly due to oxidations, with successive increases of +16 Da, consistent with multiple oxidations on the same protein molecule.

Specific amino acids have been shown to be highly susceptible to oxidation in the presence of ROS. The sulfur-containing amino acids cysteine and methionine are known to form various oxidation states including sulfenic, sulfinic and sulfonic acids for cysteines and methionine sulphoxide for methionine. [73,74] Disulfide bonds are also likely to form under oxidizing conditions. [73] To detect the presence of free thiols in non-irradiated and irradiated samples, we performed Ellman's assay. Ellman's assay utilizes the reaction of cysteine side chains with 5,5'-dithiobis-(2-nitrobenzoic acid) (DTNB) to quantify the free thiols in solution. [49,50] This assay was performed under nondenaturing conditions to assess the amounts of solvent-exposed thiols in solution. Figure 3 shows the non-irradiated sample, which has a free thiol content of 41 μM. This corresponds to 3.4 solvent-exposed thiols per protein molecule, consistent with structural analysis of the NMR and crystal structures of HγS that indicate 3 out of the 7 cysteines are highly solvent-exposed: C23, C25, and C27. [75,76] With increasing γ irradiation dose, the solvent-exposed thiol concentration decreased to 16, 13 and 9 μM after 1.5, 3.0, and 7.0 h, respectively. These concentrations correspond to 1.4, 1.1 and 0.7 solvent-exposed thiols per protein molecule for the 1.5, 3.0, and 7.0 h irradiated samples, respectively.

In general, protein oxidation via ROS has been extensively reviewed. [77] The side chains of lysine, histidine, tyrosine, tryptophan, and phenylalanine are likely targets for addition reactions: lysine residues oxidize to aminoadipic semialdehydes; [78] histidine oxidizes to asparagine, aspartic acid, and oxo-histidine; [78,79] tryptophan converts to 2-,4-,5-,6-, and 7-hydroxy-tryptophan, formylkynurenine, 3- hydroxykynurenine, and kynurenine; [80] tyrosine forms 3,4-dihydroxyphenylalanine or dityrosine crosslinks; [80] and the oxidation products of phenylalanine are 2-,3-, and 4-hydroxyphenylalanine and 3,4- dihydroxy-phenylalanine. [80] Oxidation patterns induced by hydroxyl radicals are well-characterized and predictable, leading to their use in oxidative-based footprinting methods. [81] This technique exposes proteins to hydroxyl radicals that oxidize amino acid side chains at a rate determined by solvent exposure. Side chains that are buried or involved in protein-protein interactions can be identified by their resistance to oxidation. [82] This type of footprinting is particularly useful when fast, laser-induced hydroxyl radical production is combined with modern mass spectrometry detection methods, [83] a strategy that has been used to characterize protein-peptide[84] and antibody-epitope binding, [85] among others. We expected to observe similar patterns of protein oxidation as γ irradiation produces hydroxyl radicals.

In addition to the expected oxidations, the intact mass spectra of the γ irradiated protein also indicate the presence of other modifications. We noted a spike at the 5 × oxidation state (+80); we hypothesize that an additional mass change may add +80 Da that overlaps with the 5× oxidation state. Another possibility suggested by other known PTMs is O-sulfation on serine, threonine, or tyrosine residues, although the source of SO_3 is unknown in that case. [86,87] We also observed mass losses in the irradiated samples. The resolution of the intact mass spectra makes it difficult to determine within 1 Da the exact mass of this shift; however, it appears to fall between −16 to −17 Da. There appears to be a succession of mass losses, with an apparent 1 × mass loss at −16/−17 and 2× mass loss at −33/34. The loss of

17 Da may correspond to the formation of succinimide via a sidechain nucleophilic attack on the protein backbone. Succinimide formation is readily achieved by aspartic acid which can then racemize to D-aspartic acid, [88] a common PTM in aged lenses,[89] Succinimide formation has been shown to increase in UVC irradiated α-crystallins. [90] The amount of β-linked aspartic acid, which is also formed through a succinimide intermediate, has been shown to increase in γ irradiated α-crystallins. [91] However, other modifications may overlap as well. For example, dehydroalanine formation from cysteine generates a −34 Da mass loss from the conversion of the thiol group to an olefin and has been detected as a product of protein-ROS interaction using MS/MS. [92]

In this study, we focused on the short-term mass changes and structural stability of HγS by analyzing all samples within hours of removal from the γ-irradiation source. However, intact mass spectra collected from later time points (immediately after irradiation compared to 4 hours after irradiation and 1 week after irradiation) show an increase in the amount of modified protein (Figure S2). We hypothesize that γ radiation generated ROS continue to react with the protein after removal from the energy source, consistent with previous reports that these intermediates last hours to days. [77,93]

Oxidative damage was identified on Lys, Met, Trp, Leu, and Cys

To identify the modifications, samples irradiated for 1 h/1.5 kGy were digested and analyzed with liquid chromatography tandem mass spectrometry (LC-MS/MS). This type of data-independent acquisition (DIA) allows for a less biased approach as all peptides are included in the analysis. Protein digestion was performed by proteolysis with both trypsin and pepsin on the 1.5 kGy dose samples. Trypsin digestion was performed under denaturing conditions, with the protein first incubated in 8 M urea for 1 h then diluted to 1.6 M urea for an overnight incubation with trypsin. A pepsin digest was added to increase coverage. [94] Both the trypsin and pepsin digests from 1.5 kGy samples mostly lacked distinct, identifiable peptides in the irradiated sample. This result was unexpected based on the modifications observed in the intact mass spectra of the irradiated samples. One modification was identified from the pepsin digest of the 1.5 kGy irradiated sample, the peptide GSKTGTKIF showing a −1 Da loss (Table 1). The b and y ion plots show that the location of the mass shift is in the first three residues (Figure S3). Of the three residues, lysine is the mostly likely target of oxidation. Aminoadipic semialdehyde derivatives of lysine resides are known oxidation products of lysine that yield a −1 Da loss. [95] This modification has been reported in crystallins in aged human eye lens, where its concentration increased with age and in the presence of diabetes, both conditions which increase cataract susceptibility. [96] The semialdehyde has been reported to further oxidize to the carboxylic acid derivative, 2-aminoadipic acid. [96]

The lack of unique peptides in the 1.5 kGy irradiated sample digest suggested that the modifications to HγS as a result of γ irradiation were so heterogeneous that each modified peptide has a very low individual signal, making identification of any particular species by mass spectrometry difficult. We therefore looked to increase the signal for the modified peptides by analyzing samples with longer irradiation times, 5 hours with a dose of 7.7 kGy. Additionally, we analyzed the precipitated fraction (which was not evident in the 1.5 kGy

samples) in order to observe an increased fraction of modified peptides. The water-insoluble fraction was resolubilized in denaturing buffer and subsequently digested with trypsin. Enriching the sample for modified proteins aided in identifying the sites of oxidation from radiation exposure. It should be noted that accurately measuring concentration post-exposure using UV absorption is challenging, as the UV absorption profile can change significantly due to the oxidation of the aromatic amino acids. Therefore, a direct comparison of ion count of the modified peptides between samples is not feasible as the total sample concentration may vary. In order to give an approximation of the relative amount of modified peptides between samples, we estimated the percent abundance as the ion count of the modified peptide over the total ion count of all the modified and unmodified forms of the peptide.

Table 1 summarizes the sites of oxidation identified in 7.7 kGy irradiated HγS. We found evidence of oxidation on all methionine residues and one of the four tryptophan residues. We also identified oxidation of one cysteine, C25, consistent with the high solvent exposure of this residue. The b and y ion plots supporting the identified oxidation sites are shown in the Supplementary Information, The methionine residues and W163 each show a single oxidation, with b and/or y ions demonstrating the specific position of the +16 mass addition (Figure S4-S9). We also found evidence of oxidation of leucine, with +16 mass addition to L142 (Figure S10). L133 may also be oxidized, however the b and y ions were not definitive to that position, as the +16 may also added to V132 (Figure S11). Both leucine and valine have previously been reported to form hydroperoxides and hydroxides in the presence of hydroxyl radicals and oxygen. [74] γ irradiation on a leucine-containing small peptide resulted in the formation of 4-hydroxyleucine with a +16 mass addition as a major product. [97] In contrast to the single oxidations identified for the other residues, C25 was identified as a doubly oxidized species, forming the sulfinie acid derivative. The b and y ions definitively identified C25 as doubly oxidized, rather than a single oxidation of C25 and a neighboring cysteine (Figure S12). Oxidation of methionine, tryptophan, and cysteine residues is consistent with the oxidation sites found in γE and γF in rat lenses exposed to γ irradiation. [29]

For comparison, we additionally irradiated HγS with ultraviolet (UV) radiation to determine whether similar products formed. UV radiation has been shown to directly photooxidize proteins via absorption by the major chromophoric side chains (Trp, Tyr, Phe, His, and Cys), which in turn may generate ROS and subsequently oxidize other side chains. [98,99] UV irradiation of bovine α-crystallin [90,100] and human γD (HγD) crystallin [56,101] showed oxidation of methionine, tryptophan, and cysteine residues. UVA and UVB irradiation of HγS-crystallin has previously been shown to lead to rapid formation of light-scattering, amorphous aggregates *in vitro*. [55] We performed trypsin digests on the insoluble fractions after UVA and UVB irradiation. The UV-irradiated samples show a similar pattern of oxidized amino acids, with methionines, tryptophans, and cysteines identified as oxidized products (Table 1). UV irradiated samples additionally showed that C23 and C27 formed sulfinic acid derivatives with +32 mass shifts (Figure S13 and S14). Previous studies on UV irradiated HγD report the formation of double and triple oxidized cysteines, rather than the single oxidation product. [101]

Vibrational spectroscopy reveals chemical signatures of oxidation

Infrared (IR) and Raman spectroscopy were used to gain further insight into the types of PTMs arising from γ irradiation. Both techniques are powerful approaches for directly probing vibrational signatures, and hence chemical content, of the molecules. IR spectra were collected on the non-irradiated and irradiated samples in the mid-IR region on lyophilized protein to minimize the background signal from water. Several distinct features appeared in irradiated samples (Figure 4). We noted that a peak appears at a wavelength of 2835 cm^{-1} after long irradiation times. This peak was preliminarily assigned to the C—H stretch mode of aldehydes. [102] The increase in this region in irradiated samples is consistent with the modified peptide with an aldehyde derivative of lysine identified from the mass spectrometry data. New peaks also appeared at 1373 and 1258 cm^{-1} in the spectra of irradiated samples, consistent with double bonds between sulfur and oxygen, which have a stretching mode in the 1372-1335 cm^{-1} range[102]. These data support the presence of oxidized cysteines and methionines identihed via mass spectrometry (Table 1). The peak at 1258 cm^{-1} may arise from the C—O stretching mode of carbonyl-containing functional groups. [102] Carbonyl derivatives are commonly reported in oxidized proteins and carbonyl content has been used as an indicator of oxidative stress [103,104]

Raman spectroscopy was also performed on a custom-modified Raman microscopy system. [105] Protein lines of particular interest are not strong in intensity compared to other signals within the molecular fingerprint region. To clearly observe the associated lines and changes, high concentration samples deposited on glass slides were used. [106] Due to the high protein concentration required, we first evaluated the effects of protein concentration on the modification rate from γ irradiation. We used a commercially available protein, hen egg white lysozyme, due to the significant sample consumption for high concentration samples. We obtained a non-irradiated intact mass spectrum for lysozyme, which is shown in Figure S14. We then irradiated lysozyme samples both at 5 mg/mL and 100 mg/mL for 1 h to a dose of 1.5 kGy and collected intact mass spectra. Figure S14 shows the lower concentration sample contains a much higher percentage of modified protein, consistent with ROS derived from water rather than direct irradiation of the protein causing most of the damage. We therefore chose to irradiate the HγS sample at 5 mg/mL then concentrate to 100 mg/mL for Raman data collection to maintain sample consistency between techniques.

Other reports suggest that γ irradiation may form protein peroxides, which are detectable in Raman spectra. [107,108] The HγS samples were irradiated at 5 mg/mL then concentrated with centrifugal concentrators immediately after irradiation to reach 100 mg/mL for spectra measurement. The spectra of non-irradiated sample and sample irradiated for 1.5 h 2.3 kGy is shown in Figure 5 No significant spectral changes were noted at this dose. However, we were unable to collect Raman spectra from samples with longer irradiation times due to an increase in background fluorescence. We measured this fluorescence signal at the excitation wavelength of 532 nm to determine the emission profile for the unknown fluorophore (Figure 5) To our knowledge, an amino acid derivative with this excitation-emission profile has not been reported. We aim to identify the unknown fluorescent product via further mass spectrometry analysis.

γ irradiation causes non-disulfide covalent cross-linking

In addition to the side-chain modifications noted in the previous section, γ irradiation appears to lead to chemical cross-linking between protein molecules. Figure 6 shows an SDS-PAGE of non-irradiated HγS as well as up to 1 h of irradiation or 1.5 kGy. The gels were intentionally overloaded to increase the visibility of the dimer band. During the course of irradiation, a dimer forms corresponding to approximately 40 kDa. The dimer mass is also seen in the intact mass spectra (Figure S15). HγS is known to form disulfide-bonded dimers, usually between the solvent exposed C25s in two HγS molecules. However, the dimers formed after γ irradiation resisted reduction with β-mercaptoethanol (βME), suggesting that these dimers were formed via an alternative cross-linking mechanism. Several crosslinks have been identified in aged and cataractous lenses. [109] Asp/Asn-Lys, [110] dityrosine, [111] Glu/Gln-Lys [112] have all been identified in human lenses. Dityrosine cross-linking proceeds through a radical mechanism [113] that could be promoted by irradiation and interaction with hydroxyl radical.

Longer irradiation times led to protein aggregation; however, fragmentation was not noted in either the SDS-PAGE analysis or the intact mass spectra. Figure 6 shows the SDS-PAGE of the non-irradiated protein and the irradiated protein from 1 h to 22 h. The bands for both the monomer and dimer decrease in intensity over the course of irradiation, while the band at the loading well grows more intense, suggesting that full-length protein is aggregating and no longer able to travel down the gel. By 22 h, no bands are visible in the expected mass ranges for either monomer or dimer. Neither the dimer bands nor the aggregation bands in the loading well are disrupted by reduction with βME, confirming that disulfide bonding is not the main mechanism of crosslink formation.

Conclusion

Long-lived proteins such as lens crystallins, which have evolved to maintain a stable structure for decades, are particularly vulnerable to the accumulation of detrimental modifications because they are not replenished during the human lifetime. Exposure to ionizing radiation would be expected to cause rapid protein aggregation via the large number of diverse PTMs. Remarkably, despite acquiring many modifications from exposure to γ radiation, HγS-crystallin appears to be resistant to denaturation up to very high doses. Our results clearly confirm the high tolerance for chemical modification of the γ-crystallins, highlighting their evolutionary adaptation as resilient proteins. The present study was mainly focused on the short-term structural stability of irradiated HγS. However, because cataracts often manifest many years after damage occurs, future studies should also focus on long-term structural stability.

Supplementary Material

Refer to Web version on PubMed Central for supplementary material.

Acknowledgement

The authors acknowledge Tro Babikian and John Keffer for assistance with γ irradiation in the UCI Nuclear Reactor Facility, Ben Katz and Felix Grun for management of the UCI Mass Spectrometry Facility and help with analysis, and the UCI Laser Spectroscopy Labs for access to optical instrumentation.

Funding

This work was supported by NIH grant 2R01EY021514 to R.W.M. and B.N.-B. was supported by the NSF GRFP.

References

(1). Ben-Amotz D Hydrophobic ambivalence: Teetering on the edge of randomness, J. Phys. Chem. Lett 2015, 6, 1696–1701. [PubMed: 26263336]

(2). Davis JG; Gierszal KP; Wang P; Ben-Amotz D Water structural transformation at molecular hydrophobic interfaces. Nature 2012, 491, 582–585. [PubMed: 23172216]

(3). Perera PN; Fega KR; Lawrence C; Sundstrom EJ; Tomlinson-Phillips J; Ben-Amotz D Observation of water dangling OH bonds around dissolved nonpolar groups, Proc. Natl. Acad. Sci. U. S. A 2009, 106, 12230–12234. [PubMed: 19620734]

(4). Gierszal KP; Davis JG; Hands MD; Wilcox DS; Slipchenko LV; Ben-Amotz D π-hydrogen bonding in liquid water. J. Phys. Chem. Lett 2011, 2, 2930–2933.

(5). Knapp EW; Muegge I Heterogeneous diffusion of water at protein surfaces: Application to BPTI. J. Phys. Chem 1993, 97, 11339–11343.

(6). Huang K-Y; Kingsley CN; Sheil R; Cheng C-Y; Bierma JC; Roskamp KW; Khago D; Martin RW; Han S Stability of protein-specific hydration shell on crowding. J. Am. Chem. Soc 2016, 138, 5392–5402. [PubMed: 27052457]

(7). Barnes R; Sun S; Fichou Y; Dahlquist FW; Heyden M; Han S Spatially heterogeneous surface water diffusivity around structured protein surfaces at equilibrium. J. Am. Chem. Soc 2017, 139, 17890–17901. [PubMed: 29091442]

(8). Kharakoz DP; Sarvazvan AP Hydrational and intrinsic compressibilities of globular proteins. Biopolymers 1993, 33, 11–26. [PubMed: 8427927]

(9). Khago D; Bierma JC; Roskamp KW; Kozlyuk N; Martin RW Protein refractive index increment is determined by conformation as well as composition. J. Phys.: Condens. Matter 2018, 30, 435101. [PubMed: 30280702]

(10). Ball P Water as an active constituent in cell biology. Chem. Rev 2008, 108, 74–108. [PubMed: 18095715]

(11). Tezcan FA; Crane BR; Winkler JR; Gray HB Electron tunneling in protein crystals. Proc. Natl. Acad. Sci. U. S. A 2001, 98, 5002–5006. [PubMed: 11296248]

(12). Heeker F; Stubbe J; Bennati M Detection of water molecules on the radical transfer pathway of ribonucleotide reductase by ^{17}O electron-nuclear double resonance spectroscopy. J. Am. Chem. Soc 2021, 143, 7237–7241. [PubMed: 33957040]

(13). LaVerne JA OH radicals and oxidizing products in the gamma radiolysis of water. Radiat. Res 2000, 153, 196–200. [PubMed: 10629619]

(14). Ghosal D; Omelchenko M; Gaidamakova E; V.Y. M; Vasilenko A; Venkateswaran A; Zhai M; Kostandarithes H; Brim H; Makarova K How radiation kills cells: Survival of *Deinococcus radiodurans* and *Shewanella oneidensis* under oxidative stress. FEMS Microbiol. Rev 2005, 29, 361–375. [PubMed: 15808748]

(15). Du J; Gebieki JM Proteins are major initial cell targets of hydroxyl free radicals. Int. J. Biochem. Cell Biol 2004, 36, 2334–2343. [PubMed: 15313477]

(16). Davies M; Fu S; Dean RT Protein hydroperoxides can give rise to reactive free radicals. Biochem. J 1995, 305, 643–649. [PubMed: 7832784]

(17). Robinson CK; Webb K; Kaur A; Jaruga P; Dizdaroglu M; Baliga NS; Place A; Diruggiero J A major role for nonenzymatic antioxidant processes in the radioresistance of *Halobacterium salinarum*. J. Bacteriol 2011, 193, 1653–1662. [PubMed: 21278285]

(18). Munteanu A-C; Uivarosi V; Andries A Recent progress in understanding the molecular mechanisms of radioresistance in *Deinococcus* bacteria. Extremophiles 2015, 9, 707–719.

(19). Shukla SK; Sharma AK; Bajaj S; Yashavarddhan M Radiation proteome: A clue to protection, carcinogenesis, and drug development. Drug Discovery Today 2021, 26, 525–531. [PubMed: 33137481]

(20). Lipman RM; Tripathi BJ; Tripathi EC Cataracts induced by microwave and ionizing radiation. Surv. Ophthalmol 1988, 33, 200–210. [PubMed: 3068822]

(21). Bernier M-O; Journv N; Villoing D; Doody MM; Alexander BH; Linet MS; Kitahara CM Cataract risk in a cohort of US radiologic technologists performing nuclear medicine procedures. Radiology 2018, 286, 592–601. [PubMed: 29019450]

(22). Chvlaek LT Jr; Peterson LE; Feiveson AH; Wear ML; Manuel FK; Tung WH; Hardy DS; Marak LJ; Cucinotta FA NASA study of cataract in astronauts (NASCA). Report 1: Cross-sectional study of the relationship of exposure to space radiation and risk of lens opacity. Radiat. Res 2009, 172, 10–20. [PubMed: 19580503]

(23). Nakashima E; Neriishi K; Minamoto A A reanalysis of atomic-bomb cataract data, 2000–2002: A threshold analysis. Health Phys. 2006, 90, 154–160. [PubMed: 16404173]

(24). Neriishi K; Nakashima E; Minamoto A; Fujiwara S; Akahoshi M; Mishima HK; Kitaoka T; Shore RE Postoperative cataract cases among atomic bomb survivors: Radiation dose response and threshold. Radiat. Res 2007, 168, 404–408. [PubMed: 17903036]

(25). Hammer GP; Scheidemann-Wesp U; Samkange-Zeeb F; Wicke H; Neriishi K; Blettner M Occupational exposure to low doses of ionizing radiation and cataract development: A systematic literature review and perspectives on future studies. Radiat. Environ. Biophys 2013, 52, 303–319. [PubMed: 23807741]

(26). Hamada N; Fujimichi Y; Iwasaki T; Fujii N; Furuhashi M; Kubo E; Minamino T; Nomura T; Sato H Emerging issues in radiogenic cataracts and cardiovascular disease. J. Radiat. Res 2014, 55, 831–846. [PubMed: 24824673]

(27). Cornacchia S; Errico R; La Tegola L; Maldera A; Simeone G; Fusco V; Niccoli-Asabella A; Rubini G; Guglielmi G The new lens dose limit: Implication for occupational radiation protection. La Radiologia Medica 2019, 124, 728–735. [PubMed: 30919221]

(28). Fagerholm PP; Philipson BT; Lindström B Normal human lens-the distribution of protein. Exp. Eye Res 1981, 33, 615–620. [PubMed: 7318958]

(29). Kim I; Saito T; Fujii N; Kanamoto T; Chatake T; Fujii N Site speecific oxidation of amino acid residues in rat lens γ-crystallin induced by low-dose γ-irradiation. Biochem. Biophys. Res. Commun 2015, 622–628.

(30). Ramkumar S; Fujii N; Fujii N; Thankappan B; Sakaue H; Ingu K; Natarajaseenivasan K; Anbarasu K Comparison of effect of gamma ray irradiation on wild-type and N-terminal mutants of αA-crystallin. Mol. Vision 2014, 20, 1002.

(31). Ross WM; Creighton MO; Inch WR; Trevithick JR Radiation cataract formation diminished by vitamin E in rat lenses in vitro. Exp. Eye Res 1983, 36, 645–653. [PubMed: 6852139]

(32). Ross WM; Creighton MO; Trevithick JR Radiation cataractogenesis induced by neutron or gamma irradiation in the rat lens is reduced by vitamin E. Scanning Microsc. 1990, 4, 13.

(33). Tavsi S; Memisogullari R; Koc M; Yaziei AT; Aslankurt M; Gumustekin K; Al B; Ozabaeigil F; Yilmaz A; Tahsin Ozder H Melatonin reduces oxidative stress in the rat lens due to radiation-induced oxidative injury. Int. J. Radiat. Biol 2008, 84, 803–808. [PubMed: 18979314]

(34). Morishita H; Eguehi T; Tsukamoto S; Sakamaki Y; Takahashi S; Saito C; Koyama-Honda I; Mizushima N Organelle degradation in the lens by PLAAT phospholipases. Nature 2021, 592, 634–638. [PubMed: 33854238]

(35). Bassnett S On the mechanism of organelle degradation in the vertebrate lens. Exp. Eye Res 2009, 88, 133–139. [PubMed: 18840431]

(36). Hains PG; Truseott EJ Post-translational modifications in the nuclear region of young, aged, and cataract human lenses. J. Proteome Res 2007, 6, 3935–3943. [PubMed: 17824632]

(37). Wilmarth P; Tanner S; Dasari S; Nagalla S; Riviere M; Bafna V; Pevzner P; David L Age-related changes in human crystallins determined from comparative analysis of post-translational

modifications in young and aged lens: does deamidation contribute to crystallin insolubility? J. Proteome Res 2006, 5, 2554–2566. [PubMed: 17022627]

(38). Giblin FJ Glutathione: a vital lens antioxidant. J. Ocul. Pharmacol. Ther 2000, 16, 121–135. [PubMed: 10803423]

(39). Lampi KJ; Wilmarth PA; Murray MR; David LL Lens β-crystallins: the role of deamidation and related modifications in aging and cataract. Prog. Biophys. Mol. Biol 2014, 115, 21–31. [PubMed: 24613629]

(40). Harrington V; McCall S; Huynh S; Srivastava K; Srivastava OP Crystallins in water soluble-high molecular weight protein fractions and water insoluble protein fractions in aging and cataractous human lenses. Mol. Vision 2004, 10, 476–489.

(41). Chen J; Flaugh SL; Callis PR; King J Mechanism of the highly efficient quenching of tryptophan fluorescence in human γD-crystallin. Biochemistry 2006, 45, 11552–11563. [PubMed: 16981715]

(42). Chen J; Toptygin D; Brand L; King J Mechanism of the efficient tryptophan fluorescence quenching in human γD-crystallin studied by time-resolved fluorescence. Biochemistry 2008, 47, 10705–10721. [PubMed: 18795792]

(43). Chen J; Callis PR; King J Mechanism of the very efficient quenching of tryptophan fluorescence in human γD-and γS-crystallins: the γ-crystallin fold may have evolved to protect tryptophan residues from ultraviolet photodamage. Biochemistry 2009, 48, 3708–3716. [PubMed: 19358562]

(44). Studier FW Protein production by auto-induction in high-density shaking cultures. Protein Expression Purif. 2005, 41, 207–234.

(45). Ngelale R; Lee C; Bustillos S; Nilsson M Radiolytic Degradation of Uranyl-Loaded Tributyl Phosphate by High and Low LET Radiation. Solvent Extr. Ion Exch 2019, 37, 38–52.

(46). Perry CC; Ramos-Méndez J; Milligan JR Boronated condensed DNA as a heterochromatic radiation target model. Biomacromolecules 2021, 22, 1675–1684. [PubMed: 33750108]

(47). Frieke H; Morse S The chemical action of roentgen rays on dilute ferrosulphate solutions as a measure of dose. Am. J. Roentgenol., Radium Ther. Nucl. Med 1927, 18, 430–432.

(48). Meesat R; Sanguanmith S; Meesungnoen J; Lepage M; Khalil A; Jay-Gerin J-P Utilization of the ferrous sulfate (Fricke) dosimeter for evaluating the radioprotective potential of cystamine: Experiment and Monte Carlo simulation. Radiat. Res 2012, 177, 813–826. [PubMed: 22475011]

(49). Ellman GL Tissue sulfhydryl groups. Arch. Biochem. Biophys 1959, 82, 70–77. [PubMed: 13650640]

(50). Riddles PW; Blakeley RL; Zerner B Ellman's reagent: 5, 5'-dithiobis (2-nitrobenzoic acid)–A reexamination. Anal. Biochem 1979, 94, 75–81. [PubMed: 37780]

(51). Miles A; Janes RW; Wallace BA Tools and methods for circular dichroism spectroscopy of proteins: a tutorial review. Chem. Soc. Rev 2021, 50, 8400–8413. [PubMed: 34132259]

(52). Brubaker WD; Freites JA; Golchert KJ; Shapiro RA; Morikis V; Tobias DJ; Martin RW Separating instability from aggregation propensity in γS-crystallin variants. Biophys. J 2011, 100, 498–506. [PubMed: 21244846]

(53). Pande A; Pande J; Asherie N; Lomakin A; Ogun O; King J; Benedek GB, Crystal cataracts: human genetic cataract caused by protein crystallization. Proc. Natl. Acad. Sci. U. S. A 2001, 98, 6116–6120. [PubMed: 11371638]

(54). Mandal K; Chakrabarti B; Thomson J; Siezen R Structure and stability of gamma-crystallins. Denaturation and proteolysis behavior. J. Biol. Chem 1987, 262, 8096–8102. [PubMed: 3298226]

(55). Roskamp KW; Azim S; Kassier G; Norton-Baker B; Sprague-Piercy MA; Miller ED; Martin RW Human γS-crystallin copper binding helps buffer against aggregation caused by oxidative damage. Biochemistry 2020, 59, 2371–2385. [PubMed: 32510933]

(56). Wang SS-S; Wen W-S Examining the influence of ultraviolet C irradiation on recombinant human γD-crystallin. Mol. Vision 2010, 16, 2777.

(57). Fujii N; Nakamura T; Sadakane Y; Saito T; Fujii N Differential susceptibility of alpha A-and alpha B-crystallin to gamma-ray irradiation. Biochim. Biophys. Acta, Proteins Proteomics 2007, 1774, 345–350.

(58). Vallée-Bélisle A; Michnick SW Visualizing transient protein-folding intermediates by tryptophan-scanning mutagenesis. Nat. Struct. Mol. Biol 2012, 19, 731–736. [PubMed: 22683996]

(59). Fukunaga Y; Katsuragi Y; Izumi T; Sakiyama F Fluorescence characteristics of kynurenine and N'-formylkynurenine, their use as reporters of the environment of tryptophan 62 in hen egg-white lysozyme. J. Biochem 1982, 92, 129–141. [PubMed: 7118867]

(60). Bateman AO; Sarra E; Van Genesen ST; Kappe G; Lubsen NH; Slingsby C The stability of human acidic β-crystallin oligomers and hetero-oligomers. Exp. Eye Res 2003, 77, 409–422. [PubMed: 12957141]

(61). Flaugh SL; Kosinski-Collins MS; King J Contributions of hydrophobic domain interface interactions to the folding and stability of human γD-crystallin. Protein Sci. 2005, 14, 569–581. [PubMed: 15722442]

(62). Kosinski-Collins MS; Flaugh SL; King J Probing folding and fluorescence quenching in human γD crystallin Greek key domains using triple tryptophan mutant proteins. Protein Sci. 2004, 13, 2223–2235. [PubMed: 15273315]

(63). Lampi KJ; Ma Z; Hanson SEA; Azuma M; Shih M; Shearer TR; Smith DL; Smith JB; David LL Age-related changes in human lens crystalline identified by two-dimensional electrophoresis and mass spectrometry. Exp. Eye Res 1998, 67, 31–43. [PubMed: 9702176]

(64). Forsythe HM; Vetter CJ; Jara KA; Reardon PN; David LL; Barbar EJ; Lampi KJ Altered protein dynamics and increased aggregation of human γS-crystallin due to cataract-associated deamidations. Biochemistry 2019, 58, 4112–4124. [PubMed: 31490062]

(65). Vetter CJ; Thorn DC; Wheeler SG; Mundorff CC; Halverson KA; Wales TE; Shinde UP; Engen JR; David LL; Carver JA Cumulative deamidations of the major lens protein γS-crystallin increase its aggregation during unfolding and oxidation. Protein Sci. 2020, 29, 1945–1963. [PubMed: 32697405]

(66). Hains PG; Truseott RJ Proteomic analysis of the oxidation of cysteine residues in human age-related nuclear cataract lenses. Biochim. Biophys. Acta, Proteins Proteomics 2008, 1784, 1959–1964.

(67). Linetsky M; Ortwerth B Quantitation of the singlet oxygen produced by UVA irradiation of human lens proteins. Photochem. Photobiol 1997, 65, 522–529. [PubMed: 9077138]

(68). Zigman S Environmental near-UV radiation and cataracts. Optom. and Vis. Sci 1996, 3, 182.

(69). Gutteridge JM; Wilkins S Copper salt dependent hydroxyl radical formation damage to proteins acting as antioxidants. Biochim. Biophys. Acta, Gen. Subj 1983, 759, 38–41.

(70). Halliwell B; Gutteridge JM The antioxidants of human extracellular fluids. Arch. Biochem. Biophys 1990, 280, 1–8. [PubMed: 2191627]

(71). Gunther MR; Hanna PM; Mason RP; Cohen MS Hydroxyl radical formation fron cuprous ion and hydrogen peroxide: A spin-trapping study. Arch. Biochem. Biophys 1995, 316, 515–522. [PubMed: 7840659]

(72). Barnham KJ; Masters CL; Bush AI Neurodegenerative diseases and oxidative stress. Nat. Rev. Drug Discovery 2004, 3, 205–214. [PubMed: 15031734]

(73). Alcock LJ; Perkins MV; Chalker JM Chemical methods for mapping cysteine oxidation. RIC Reviews 2018, 47, 231–268.

(74). Dean RT; FU S; Socker R; Davies MJ Biochemistry and pathology of radical-mediated protein oxidation. Biochem. J 1997, 324, 1–18. [PubMed: 9164834]

(75). Kingsley CN; Brubaker WD; Markovic S; Diehl A; Brindley AJ; Osehkinat H; Martin RW Preferential and specific binding of human αB-crystallin to a cataract-related variant of γS-crystallin. Structure 2013, 21, 2221–2227. [PubMed: 24183572]

(76). Thorn DC; Grosas AB; Mabbitt PD; Ray NJ; Jackson CJ; Carver JA The structure and stability of the disulfide-linked γS-crystallin dimer provide insight into oxidation products associated with lens cataract formation. J. Mol. Biol 2019, 431, 483–497. [PubMed: 30552875]

(77). Davies MJ Protein oxidation and peroxidation. Biochem. J 2016, 473, 805–825. [PubMed: 27026395]

(78). Uchida K Histidine and lysine as targets of oxidative modification. Amino Acids 2003, 25, 249–257. [PubMed: 14661088]

(79). Yong SH; Karel M Reactions between peroxidizing lipids and histidyl residue analogues: Enhancement of lipid oxidation and browning by 4-methylimidazole. Lipids 1978, 13, 1–5. [PubMed: 24161]

(80). Stadtman ER; Levine RL Chemical modification of proteins by reactive oxygen species; John Wiley & Sons Hoboken NJ, 2006; Vol, 9; pp 1–23.

(81). Xu G; Chance MR Hydroxyl radical-mediated modification of proteins as probes for structural proteomics. Chem. Rev 2007, 107, 3514–3543. [PubMed: 17683160]

(82). Xu G; Takamoto K; Chance MR Radiolytic Modification of Basic Amino Acid Residues in Peptides: Probes for Examining Protein- Protein Interactions. Anal. Chem 2003, 75, 6995–7007. [PubMed: 14670063]

(83). Johnson DT; Di Stefano LH; Jones LM Fast photochemical oxidation of proteins (FPOP): A powerful mass spectrometry–based structural proteomics tool. J. Biol. Chem 2019, 294, 11969–11979. [PubMed: 31262727]

(84). Zhang H; Gau BC; Jones LM; Vidavsky I; Gross ML Fast photochemical oxidation of proteins for comparing structures of protein- ligand complexes: the calmodulin- peptide model system. Anal. Chem 2011, 83, 311–318. [PubMed: 21142124]

(85). Jones LM; B. Sperry J; A. Carroll J; Gross ML Fast photochemical oxidation of proteins for epitope mapping. Anal. Chem 2011, 83, 7657–7661. [PubMed: 21894996]

(86). Woods AS; Wang H-YJ; Jackson SN Sulfation, the Up-and-Coming Post-Translational Modification: Its Role and Mechanism in Protein- Protein Interaction. J. Proteome Res 2007, 6, 1176–1182. [PubMed: 17256885]

(87). Medzihradszky KF; Darula Z; Perlson E; Fainzilber M; Chalkley RJ; Ball H; Greenbaum D; Bogyo M; Tyson DR; Bradshaw RA; Burlingame AL O-sulfonation of serine and threonine: Mass spectrometric detection and characterization of a new posttranslational modification in diverse proteins throughout the eukaryotes. Mol. Cell. Proteomics 2004, 3, 429–440. [PubMed: 14752058]

(88). Aswad DW; Paranandi MV; Sehurter BT Isoaspartate in peptides and proteins: Formation, significance, and analysis. J. Pharm. Biomed. Anal 2000, 21, 1129–1136. [PubMed: 10708396]

(89). Warmack R; Shawa H; Liu K; Lopez K; Loo J; Horwitz J; Clarke S The L-isoaspartate modification within protein fragments in the aging lens can promote protein aggregation. J. Biol. Chem 2019 , 294, 12203–12219. [PubMed: 31239355]

(90). Fujii N; Uchida H; Saito T The damaging effect of UV-C irradiation on lens alpha-crystallin. Mol. Vision 2004, 10, 814–820.

(91). Fujii N; Hiroki K; Matsumoto S; Masuda K; Inoue M; Tanaka Y; Awakura M; Akaboshi M Correlation between the loss of the chaperone-like activity and the oxidation, isomerization and racemization of gamma-irradiated α-crystallin. Photochem. Photohiol 2001, 74, 477–482.

(92). Kim H-J; Ha S; Lee HY; Lee K-J ROSics: Chemistry and proteomics of cysteine modifications in redox biology. Mass Spectrom. Rev 2015, 34, 184–208. [PubMed: 24916017]

(93). Gebicki S; Gebicki JM Formation of peroxides in amino acids and proteins exposed to oxygen free radicals. Biochem. J 1993, 289, 743–749. [PubMed: 8435071]

(94). Lakbub JC; Shipman JT; Desaire H Recent mass spectrometry-based techniques and considerations for disulfide bond characterization in proteins. Anal. Bioanal. Chem 2018, 410, 2467–2484. [PubMed: 29256076]

(95). Requena JR; Chao C-C; Levine RL; Stadtman ER Glutamic and aminoadipic semialdehydes are the main carbonyl products of metal-catalyzed oxidation of proteins. Proc. Natl. Acad. Sci. U. S. A 2001, 98, 69–74. [PubMed: 11120890]

(96). Fan X; Zhang J; Theves M; Strauch C; Nemet I; Liu X; Qian J; Giblin FJ; Monnier VM Mechanism of lysine oxidation in human lens crystallins during aging and in diabetes. J. Biol. Cherri 2009 , 284, 34618–34627.

(97). Sharp JS; Tomer KB Effects of anion proximity in peptide primary sequence on the rate and mechanism of leucine oxidation. Anal Chem. 2006 , 78, 4885–4893. [PubMed: 16841907]

(98). Davies MJ; Truseott EJ Photo-oxidation of proteins and its role in cataractogenesis. J. Photochem. Photobiol., B 2001, 63, 114–125. [PubMed: 11684458]

(99). Davies MJ Singlet oxygen-mediated damage to proteins and its consequences. Biochem. Biophys. Res. Commun 2003, 305, 761–770. [PubMed: 12763058]

(100). Finley EL; Busman M; Dillon J; Crouch EK; Sehev KL Identification of photooxidation sites in bovine α-crystallin. Photochem. Photobiol 1997, 66, 635–641. [PubMed: 9383987]

(101). Sehafheimer N; Wang Z; Sehey K; King J Tyrosine/cysteine cluster sensitizing human γD-crystallin to ultraviolet radiation-induced photoaggregation in vitro. Biochemistry 2014, 53, 979–990. [PubMed: 24410332]

(102). Segneanu AE; Gozeseu I; Dabiei A; Sfirloaga P; Szabadai Z Macro to nano spectroscopy, InTechOpen: Rijeka, 2012; Vol, 145; pp 145–164.

(103). Amici A; Levine R; Tsai L; Stadtman E Conversion of amino acid residues in proteins and amino acid homopolymers to carbonyl derivatives by metal-catalyzed oxidation reactions. J. Biol. Chem 1989 , 264, 3341–3346. [PubMed: 2563380]

(104). Moskovitz J; Oien DB Protein carbonyl and the methionine sulfoxide reductase system. Antioxid. Redox Signaling 2010, 12, 405–415.

(105). Liu Y; Asset T; Chen Y; Murphy E; Potma EO; Matanovic I; Fishman DA; Atanassov P Facile all-optical method for in situ detection of low amounts of ammonia. Iscience 2020, 23, 101757. [PubMed: 33241202]

(106). Zhang D; Xie Y; Mrozek MF; Ortiz C; Davisson VJ; Ben-Amotz D Raman detection of proteomic analytes. Anal. Chem 2003 , 75, 5703–5709. [PubMed: 14588009]

(107). Zbikowska HM; Nowak P; Waehowiez B Protein modification caused by a high dose of gamma irradiation in cryo-sterilized plasma: Protective effects of ascorbate. Free Radical Biol. Med 2006, 40, 536–542. [PubMed: 16443169]

(108). Sjöberg B; Foley S; Cardey B; Fromm M; Eneseu M Methionine oxidation by hydrogen peroxide in peptides and proteins: A theoretical and Raman spectroscopy study. J. Photochem. Photobiol., B 2018, 188, 95–99. [PubMed: 30240974]

(109). Sehey KL; Wang Z; Friedrich M; Truscott RJ New insights into the mechanisms of age-related protein-protein crosslinking in the human lens. Exp. Eye Res 2021, 108679. [PubMed: 34147508]

(110). Friedrich MG; Wang Z; Sehey KL; Truscott RJ Spontaneous cross-linking of proteins at aspartate and asparagine residues is mediated via a succinimide intermediate. Biochem. J 2018, 475, 3189–3200. [PubMed: 30181147]

(111). Giulivi C; Traaseth NJ; Davies KJA Tyrosine oxidation products: Analysis and biological relevance. Amino Acids 2003, 25, 227–232. [PubMed: 14661086]

(112). Friedrich MG; Wang Z; Sehey KL; Truscott RJ Spontaneous protein–protein crosslinking at glutamine and glutamic acid residues in long-lived proteins. Biochem. J 2021, 478, 327–339. [PubMed: 33345277]

(113). Heinecke JW; Li W; Francis GA; Goldstein JA Tyrosyl radical generated by myeloperoxidase catalyzes the oxidative cross-linking of proteins. J. Clin. Invest 1993, 91, 2866–2872. [PubMed: 8390491]

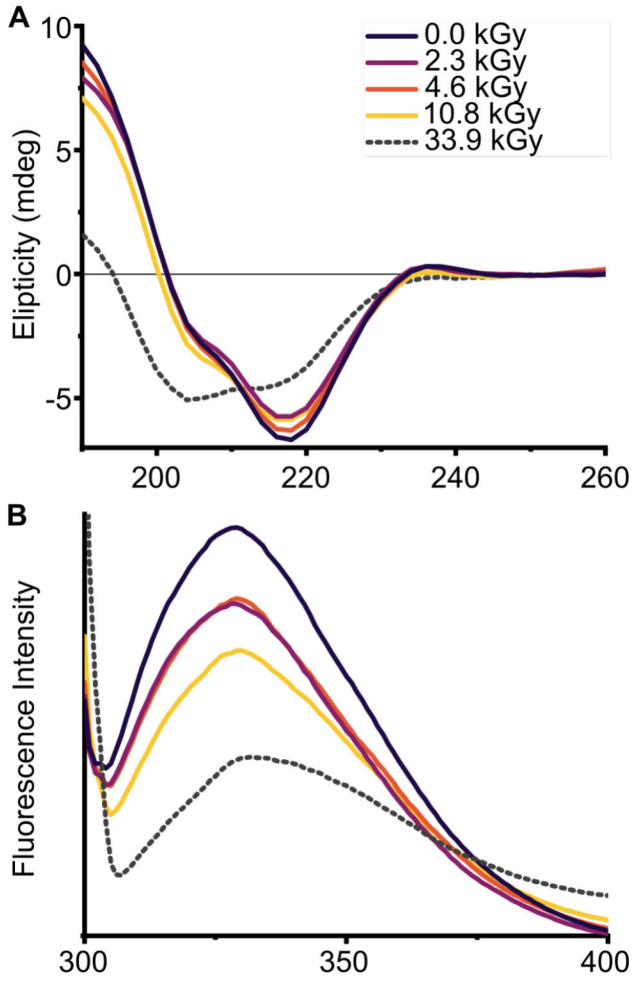

Figure 1:

The structure of HγS was monitored using circular dichroism (CD) and intrinsic tryptophan fluorescence spectroscopy. (A) CD and (B) fluorescence spectra of HγS irradiated from 0 kGy (black), 2.3 kGy (purple) 4.6 kGy (orange), 10.8 kGy (yellow), 33.9 kGy (grey, dashed). HγS resists significant secondary structural rearrangement past 10.8 kGy.

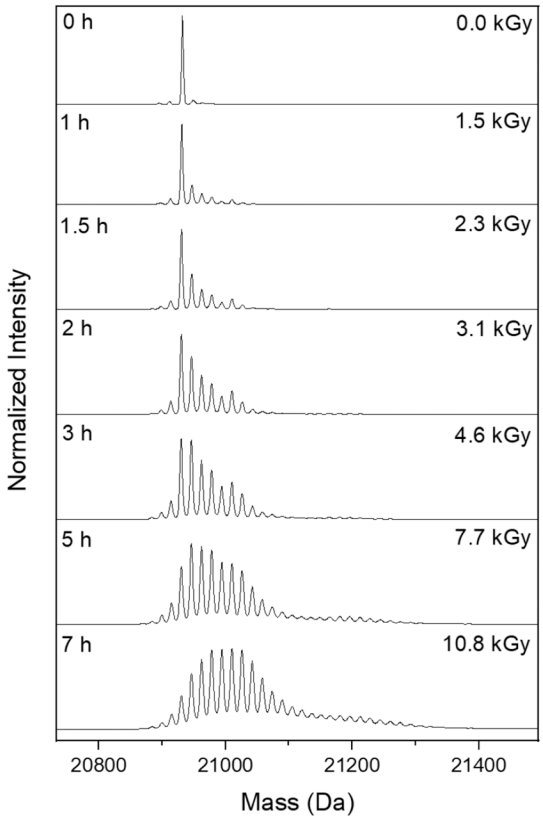

Figure 2:

Deconvoluted intact mass spectra HγS samples irradiated with doses (0, 1.5, 2.3, 3.1, 4.6, 7.7, and 10.8 kGy) of γ radiation. HγS accumulates successive +16 Da and −16/−17 Da modifications over the course of irradiation.

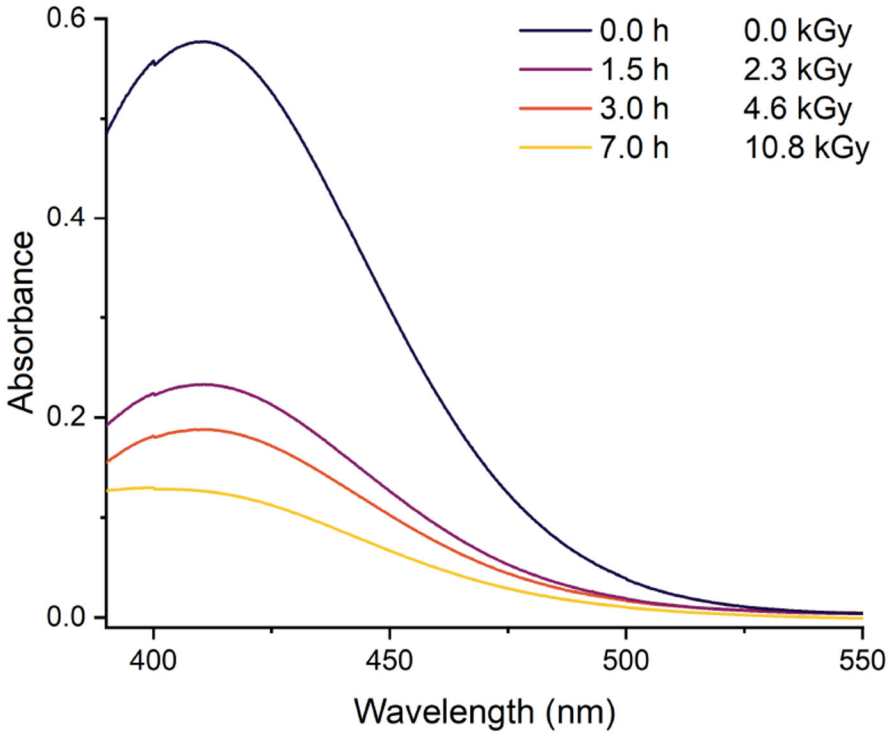

Figure 3:

Absorbance spectra of non-irradiated and irradiated samples after reaction with Ellman's reagent, DTNB. The absorbance at 412 nm was used to calculate the concentration of free thiols.

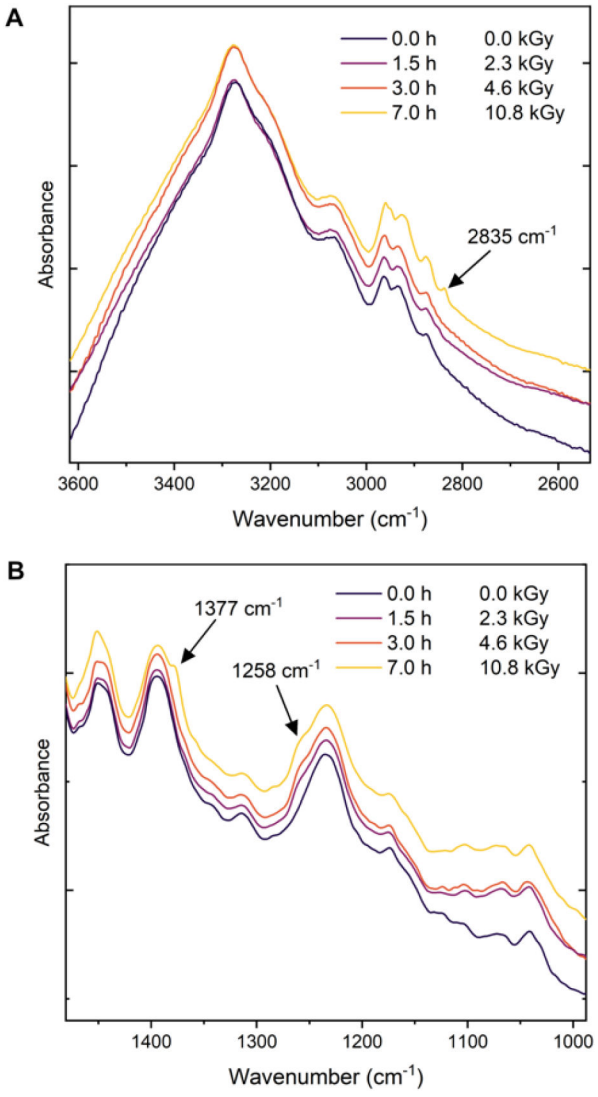

Figure 4:

IR spectra for samples irradiated from 0.0 to 10.8 kGy from (A) 3655 to 2520 cm^{-1} and (B) 1480 to 990 cm^{-1}. Traces are offset for clarity. Unique peaks that appear after irradiation are indicated with an arrow.

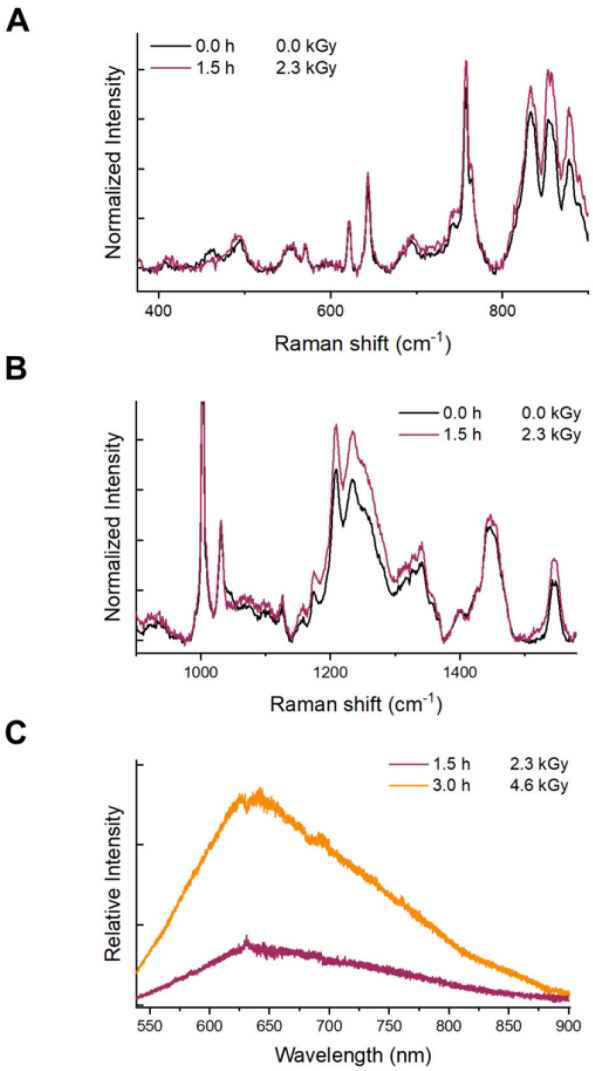

Figure 5:

Raman spectra of non-irradiated and irradiated HγS from (A) 375 to 900 cm^{-1} and (B) 900 to 1580 cm^{-1}. No significant spectral changes are observed from 1 h/1.5 kGy dose. (C) Fluorescence spectra of irradiated HγS with an excitation wavelength of 532 nm.

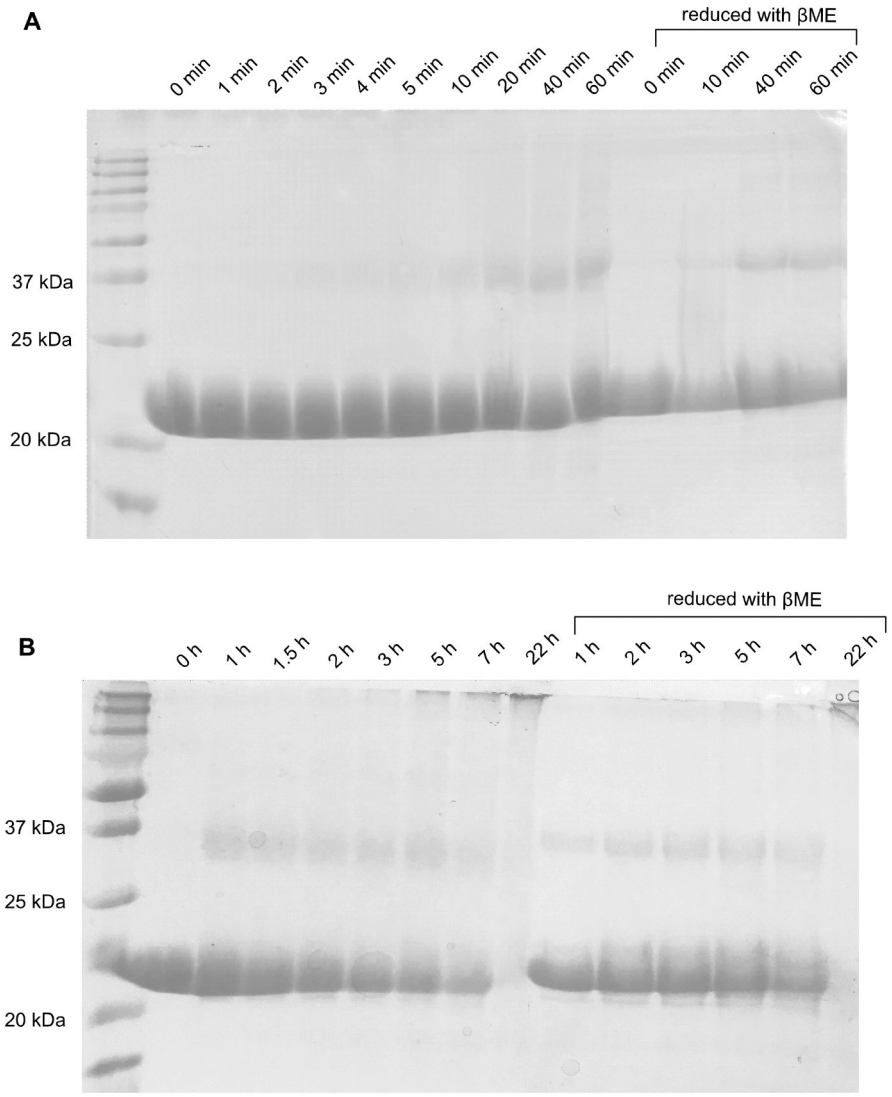

Figure 6:

SDS-PAGE analysis of non-irradiated and irradiated HγS. (A) Short γ irradiation exposures from 0 to 60 min, up to 1.5 kGy. A dimer of HγS forms that resists reduction with βME. (B) Longer γ irradiation exposures from 0 to 22 h, up to 33.9 kGy. Aggregation appears to increase with longer irradiation times with no remaining monomer or dimer visible at 22 h.

Table 1.

Oxidation sites identified in γ and UV irradiated HγS. Peptides from pepsin and trypsin digests were separated and identified via LC-MS/MS. The percent abundance is calculated from the ion count of the modified peptide over the total ion count of all modified and unmodified forms of the peptide. No data is available on the presence of the $K3^{-1}$ modification of GSKTGTKIF as pepsin digests were not performed for the 7.7 kGy γ irradiated or UV irradiated samples. The unmodified form of GSKTGTKIF was not detected; therefore, percent abundance is not reported.

Residue Number	Peptide	Modification	Nonirradiated	γ-rays		UV	
				1.5 kGy	7.7 kGy	UVA	UVB
1-10	GS**K**TGTKITF	$K3^{-1}$	nd	detected[a,b]	-	-	-
42-72	VEGGTWAVYERPNFAGY**M**YILPQGEYPEYQR	$M59^{+16}$	nd	nd	16%	8%	14%
73-79	W**M**GLNDR	$M74^{+16}$	nd	nd	3%	2%	3%
102-125	GDFSGQ**M**YETTEDCPSI**M**EQFH**M**R	$M108^{+16}$	nd	nd	5%	7%	10%
		$M119^{+16}$	nd	nd	8%	11%	11%
		$M124^{+16}$	nd	nd	2%	6%	9%
132-146	**VL**EGVWIFYE**L**PNYR	$V132^{+16}$ or $L133^{+16}$	nd	nd	1%[b]	nd	nd
		$L142^{+16}$	nd	nd	< 1%	nd	nd
159-174	KPID**W**GAASPAVQSFR	$W163^{+16}$	nd	nd	< 1%	< 1%	< 1%
20-36	RYD**C**D**C**D**C**ADFHTYLSR	$C23^{+32}$	nd	nd	nd	2%	3%
		$C25^{+32}$	nd	nd	1%	4%	8%
		$C27^{+32}$	nd	nd	nd	< 1%	1%

nd = not detected

[a] percentage not reported as unmodified peptide uot detected

[b] Assignment of oxidation to specific residue not definitive